ISSN 0023-1584, Kinetics and Catalysis, 2011, Vol. 52, No. 2, pp. 157–165. © Pleiades Publishing, Ltd., 2011.
Original Russian Text © V.A. Pavlov, O.P. Shatalov, 2011, published in Kinetika i Kataliz, 2011, Vol. 52, No. 2, pp. 163–172.

Measuring the Ignition Delay Time for Hydrogen–Oxygen Mixtures behind the Front of an Incident Shock Wave

V. A. Pavlov and O. P. Shatalov

Institute of Mechanics, Moscow State University, Moscow, 119991 Russia

e-mail: pavlov@imec.msu.ru

Received November 26, 2009

Abstract—The delay time τ has been measured for the formation of the ·OH radical in igniting hydrogen–oxygen mixtures diluted with argon (79–97%). The experiments have been carried out under incident shock wave conditions at temperatures of 900–3000 K, pressures of 0.5–2.5 atm, and H_2/O_2 ratios of 0.2–20. The dependence of τ on the pressure P_s of the stoichiometric part of the combustible mixture ($2H_2–O_2$) has been investigated for different mixture compositions. Under the above conditions, τ depends practically linearly on $1/P_s$ at $P_s = 0.02–0.1$ atm, irrespective of the mixture composition. This allows the measured τ data to be converted to one quantity, τP_s. The temperature dependence of τP_s in the P_s range from 0.02 to 0.1 atm is Arrhenius-like. For the hydrogen-rich mixtures ($H_2/O_2 = 2–20$), this dependence appears as $\tau P_s = 0.057 + 0.0256\exp(7470/T)$ μs atm; for the lean mixtures ($H_2/O_2 = 0.125–1$), $\tau P_s = 0.021 + 0.0069\exp(7470/T)$ μs atm. The length of the shock-heated gas plug in the incident shock wave poses limitations on the ignition delay time measurements at $T < 900$ K.

DOI: 10.1134/S0023158411020157

The combustion of hydrogen–oxygen mixtures has been the subject of many studies; nevertheless, the ignition, combustion, and detonation mechanisms are still not understood in detail. Although the theory of hydrogen–oxygen combustion has been developed rather well [1–3], many phenomena observed in this process still remain unexplained. While the $H_2–O_2$ system is comparatively simple, its branched chain ignition involves a wide variety of molecules, atoms, and radicals in the ground and excited states. A kinetic model of this process may include a large number of chemical reactions, and the rate constant data for many of them are insufficiently reliable. For this reason, when comparing calculated and experimental data, one has to adjust the values of "unreliable" constants. This often allows these data to be reconciled for some process conditions (temperature, pressure, mixture composition, etc.) while leading to marked discrepancies for other conditions. An important characteristic of the ignition of a combustible mixture is the ignition delay time τ (induction period). The quality of an ignition model is often judged from the goodness of fit between the calculated and measured τ values. It is, therefore, necessary to accumulate extensive ignition delay data measured under various conditions.

In most studies on the ignition delay for hydrogen–oxygen mixtures, measurements have been taken in incident or reflected shock waves over wide temperature, pressure, mixture composition, and buffer gas dilution factor ranges. The attractiveness of shock tubes in these experiments is explained by the formation of a "plug" of an instantaneously heated gas throughout the tube cross section behind the front of the incident shock wave. However, even experimental data obtained at the same temperature, pressure, and mixture composition may differ by a factor of 2–3 or larger. This is possibly due to the difference between experimental techniques and between gas dynamic conditions. It is the necessity of verifying and refining the existing experimental data that prompted us to carry out this study.

Here, we report ignition delay measurements for hydrogen–oxygen mixtures in a shock tube over wide temperature, pressure, and component concentration ranges. We attempt to establish correlations and find conditions for setting up an analytical expression for τ as a function of temperature and pressure.

The ignition delay time was determined as the delay of the onset of light emission from the electronically excited ·OH* radical relative to the front of the initiating shock wave. We chose light emission from the ·OH* radical for our measurements for the reason that it appears at the early stages of mixture combustion. We studied $H_2–O_2$ mixtures diluted with argon (79–97%) at temperatures of 900–3000 K, pressures of 0.5–2.5 atm, and H_2/O_2 ratios of 0.2–20 (by pressure).

EXPERIMENTAL

Experiments were carried out in a shock tube with an inner diameter of 57 mm. The experimental setup had a vacuum pumping system, a gas preparation and admission system, emission and absorption spectro-

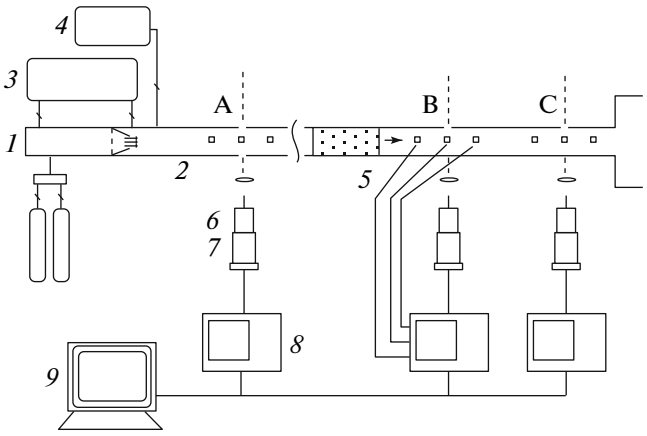

Fig. 1. Experimental setup: (*1*) high-pressure section, (*2*) low-pressure section. (*3*) pumping system, (*4*) gas blender, (*5*) piezoelectric sensors, (*6*) spectrograph, (*7*) photomultiplier, (*8*) oscilloscope, and (*9*) computer. A, B, and C are the observation cross sections.

scopic equipment, and shock wave velocity and pressure profile measuring devices (Fig. 1).

The shock tube consisted of a 1-m-long high-pressure section and a 4.5-m-long low-pressure section separated by a diaphragm. The low-pressure section was filled with the gas to be examined; the high-pressure section, with a driver gas. The tube was vacuumized with a fore pump and a turbomolecular pump, which allowed the residual pressure of 10^{-4} Torr to be maintained in the system. Gas leakage into the low-pressure section because of its imperfect tightness did not exceed 10^{-4} Torr/min. The error associated with the filling of the tube with the gas mixture to be examined, with a preset composition and pressure, was not larger than 0.5%.

The burst of the diaphragm gave rise to a propagating shock wave in the low-pressure section, which compressed and heated the gas examined. Gas mixtures were prepared in a stainless steel airtight 40-l gas blender at a pressure of 1 atm. This was done using an IPDTs-1 digital pressure sensor accurate to 0.1 Torr. The initial pressure of the mixture in the low-pressure section was 45–90 Torr in all runs. The driver gas was helium. For finer adjustment of shock wave parameters, nitrogen was added to the gas in the high-pressure section. The gas dynamic parameters at the shock front were calculated for each particular run from the measured shock wave velocity and the initial parameters of the mixture using the Gaseq program.

The shock wave velocity and gas pressure distribution in the wave were determined using piezoelectric ceramic sensors with a resonance frequency of 300 kHz and sensing element diameter of 1 mm. The sensors were mounted symmetrically in the shock tube wall on both sides of the observation cross section, each 5 cm away from it. The sensitivity of the sensors was ~0.3 W/atm. In the observation cross section, there were quartz windows for light inlet/outlet and a piezoelectric sensor for monitoring the pressure variation in this cross section. The signals from the piezoelectric sensors and radiation from the shock tube were recorded with Tektronix TDS 3014 and Agilent 54624A quad beam oscilloscopes with a bandpass width of 100 MHz, both coupled to a PC. The error in the shock wave velocity measurements was ~0.5%, and it was mainly determined by the accuracy of measuring the distance between the sensing elements of the piezoelectric sensors.

The light emitted from the gas behind the shock front in the observation cross section was focused on the entrance slit of an MS-300 diffraction spectrograph with a focal distance of 0.3 m and was detected with an FEU-100 photomultiplier placed in the exit focal plane of the spectrograph. Chemiluminescence was measured at a wavelength of 306.4 nm ($A^2\Sigma^+ \longleftrightarrow X^2\Pi$ transition) in a spectral interval of 10 nm, which covered the "head" of the emission band of the $^{\cdot}$OH radical. The time resolution of the spectroscopic channel was ~0.7 μs and was determined by the geometry of the optical scheme. The actual length of the shock-compressed gas plug was determined by recording the time sweep of light absorption by dioxygen at $\lambda = 220$ nm (Schumann–Runge band).

A specific feature of the shock tube was that it had three identical measurement sections, whose central cross sections were located at a distance of 2.4 m (cross section A), 4.0 m (B), and 4.2 m (C) from the diaphragm. By measuring the velocity of the emitting zone in the two neighbor sections B and C, it was possible to judge the character of combustion wave propagation inside the shock-compressed gas plug and to exclude the accelerating combustion modes from consideration.

Figure 2 presents a typical oscillogram of the signals from the piezoelectric sensors (curve *1*) and light emission from the $^{\cdot}$OH radical (curve *2*) in the measurement cross sections B and C for the ignition of the 1% O_2 + 4% H_2 + 95% Ar mixture. The shock wave velocity was $V = 1.04$ km/s, the gas temperature at the shock front was $T = 1177$ K, and the pressure was $P = 1.48$ atm.

RESULTS AND DISCUSSION

Ignition delay data for different mixture and the corresponding shock wave parameters are presented in the table. The maximum emission time data are also included in the table for the reason that some model calculations have been carried out in terms of the maximum $^{\cdot}$OH concentration time (see, e.g., [4–6]).

Because of the specific features of experiments in shock tubes, the ignition delay time τ at different temperatures depends on the gas pressure behind the shock wave. In most cases, τ values measured for the

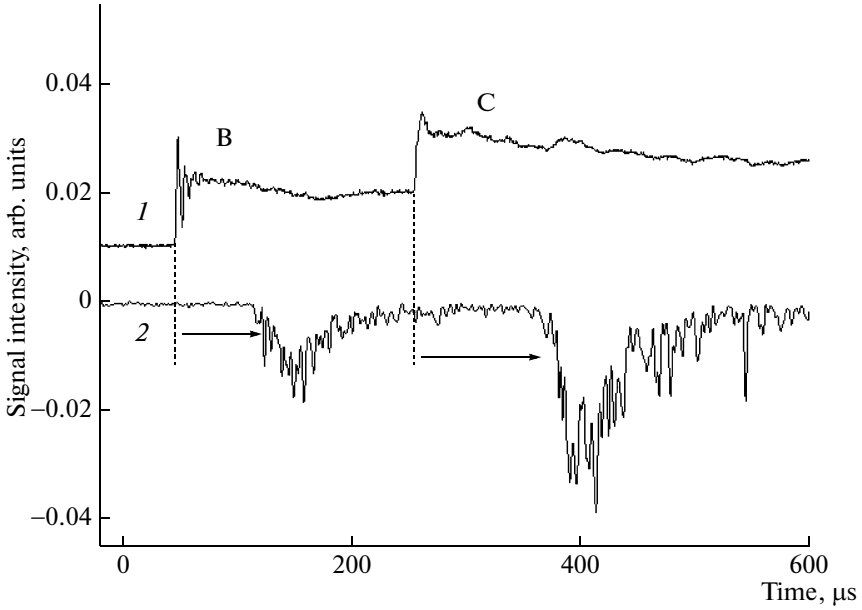

Fig. 2. Time sweeps of the (*1*) pressure and (*2*) $^{\bullet}$OH emission signals in the cross sections B and C of the shock tubes.

same mixture at the same temperature but at different pressures vary significantly. An analysis of the τ data obtained in this work demonstrated that there is a nearly linear correlation between the delay time and the total pressure for a given mixture composition. This allowed the measured τ values to be converted to normal pressure.

The τP values (P = gas pressure behind the shock wave) measured in this study and the same values calculated from data of other authors [7, 8] for the same mixtures and different pressures are in good agreement. However, there is no agreement between the τP data obtained for mixtures differing in the concentration of either argon or reactants. At the same time, having introduced the concept of the pressure of the stoichiometric part of the combustible mixture (P_s), we observed the same $\tau \sim 1/P_s$ dependence for $P_s \leq 0.1$ atm both for the data of this study and for the data of other authors [7–11] converted to τP_s.

Now we will explain the term "pressure of the stoichiometric part of the combustible mixture" using the following example: in the 1% O_2 + 20% H_2 + 79% Ar mixture, the stoichiometric part ($2H_2 + O_2$) accounts for 3% and, at a total pressure of 5 atm, $P_s = 0.15$ atm.

Figure 3 shows the temperature dependences of the ignition delay τP_s converted to normal pressure for H_2–O_2–Ar mixtures according to this work and other studies [7–11]. The P_s and P values did not exceed 0.1 and 64 atm, respectively. The H_2/O_2 concentration ratio was between 20 and 0.125. The Ar concentration was 99.85–70.00%. It is clear from Fig. 3 that all τP_s data can be divided into three groups. One group pertains to rich and near-stoichiometric mixtures with H_2/O_2 = 1–20 (dependence *1*). The second group characterizes lean mixtures with H_2/O_2 = 0.125–0.5 (dependence *2*). For both groups, the temperature dependence of τP_s is Arrhenius-like. The approximating formula for the rich and stoichiometric mixtures is

$$\tau P_s = 0.057 + 0.0256\exp(7470/T)\ \mu\text{s atm}, \quad (1)$$

for the lean mixtures,

$$\tau P_s = 0.021 + 0.0069\exp(7470/T)\ \mu\text{s atm}. \quad (2)$$

The τP_s values for the lean mixtures are 2–5 times smaller than those for the mixtures containing excess hydrogen; that is, the lean mixtures ignite substantially more rapidly. The maximum deviation between the measured τP_s values and the values defined by expression (1) for rich mixtures is 15–20%. For lean mixtures, the ignition delay time lengthens markedly as the O_2/H_2 ratio is increased. However, even in this case expression (2) provides a τP_s estimate accurate to at least 50%.

The practically linear dependence of τ on inverse stoichiometric pressure at $P_s < 0.1$ atm, irrespective of the mixture composition, indicates that ignition under these conditions is nearly binary. In this study, as distinct from our previous work [14], we compare our data and the data of other researchers [7, 8] to the τP_s values calculated from the data reported in [9, 12, 13] for wider ranges of P_s (0.05–0.44 atm) and P (1–7 atm) for rich mixtures (Fig. 4). Throughout the temperature range examined, at $P_s < 0.1$ atm the data being compared are in good agreement. At $P_s > 0.1$ atm, $P > 2$ atm, and $T \approx 1000$ K, significant discrepancies are observed: as the total pressure and partial stoichiometric pressure

Delay time data for the ignition of hydrogen–oxygen mixtures in shock tubes and shock wave parameters

Entry	P_0, atm	V, km/s	T, K	P_2, atm	ρ/ρ_0	τ_{lab}, μs	τ_{act}, μs	τ_{lab}^{max}, μs	τ_{act}^{max}, μs	P_s, atm	$\tau_{act}P_s$, μs atm
3% ($1O_2 + 2H_2$) + 97% Ar											
1	0.12	0.845	878	0.98	2.8	1000	2800			0.0294	82.32
2	0.12	0.86	903	1.02	2.84	760	2160			0.0306	66.1
3	0.12	0.87	913	1.04	2.9	808	2343	870	2523	0.0312	73
4	0.12	0.9	963	1.12	2.9	650	1885	730	2117	0.0336	63.3
5	0.06	0.96	1060	0.64	3.01	414	1246	490	1475	0.0192	23.9
6	0.06	0.98	1095	0.67	3.04	316	960	382	1160	0.0201	19.3
7	0.06	0.99	1108	0.68	3.04	290	880	328	997	0.0204	17.9
8	0.06	1.03	1183	0.74	3.1	178	552	219	680	0.0222	12.2
9	0.06	1.05	1220	0.77	3.15	142	447	182	573	0.0231	10.3
10	0.06	1.1	1313	0.84	3.2	96	307	111	355	0.0252	7.1
11	0.06	1.18	1472	0.97	3.3	57	188	111	366	0.0291	5.47
12	0.06	1.24	1596	1.1	3.38	30	101	45	152	0.033	3.33
5% ($1O_2 + 2H_2$) + 95% Ar											
13	0.06	0.84	858	0.48	2.8	1080	3025	1160	3248	0.024	72.6
14	0.06	1.037	1175	0.74	3.14	154	484	196	615	0.037	17.9
15	0.06	1.037	1176	0.74	3.15	150	472	170	535	0.037	17.5
16	0.06	1.077	1247	0.8	3.19	86	274	111	354	0.04	10.96
17	0.06	1.196	1477	0.99	3.35	36	120.6	40	134	0.0495	5.97
18	0.06	1.33	1764	1.23	3.48	13.6	47	22.4	78	0.0615	2.89
19	0.06	1.39	1902	1.34	3.53	9.2	32.5	16.4	58	0.067	2.18
8% ($1O_2 + 1H_2$) + 92% Ar ($2H_2 + O_2$) = 6%											
20	0.06	0.84	845	0.48	2.82	870	2453	900	2540	0.0288	70.6
21	0.06	0.87	888	0.5	2.9	732	2117	794	2300	0.03	63.5
22	0.06	1.05	1170	0.76	3.2	80	256	96	308	0.0456	11.7
23	0.06	1.059	1192	0.77	3.21	79	254	94	301	0.0462	11.73
24	0.06	1.055	1186	0.76	3.23	74	239	92	297	0.0456	10.9
25	0.12	1.059	1193	1.54	3.23	41.2	133	48.4	156	0.0924	12.3
26	0.12	1.059	1193	1.54	3.23	42.4	137	50	161	0.0924	12.6
27	0.06	1.06	1194	0.77	3.23	70	226	90	290	0.0462	10.4
28	0.06	1.082	1234	0.8	3.26	57	186	74	241	0.048	8.9
29	0.06	1.087	1242	0.81	3.26	53	173	71	228	0.0486	8.4
30	0.06	1.096	1260	0.82	3.27	51	167	63	206	0.0492	8.2
31	0.06	1.1	1270	0.8	3.28	47	154	65	213	0.048	7.4
32	0.12	1.12	1303	1.72	3.28	23	75	29	95	0.1032	7.74
33	0.06	1.136	1333	0.9	3.33	34	113	46	153	0.054	6.1
34	0.06	1.207	1470	1.0	3.45	20	70	30	103	0.06	4.2
35	0.06	1.21	1480	1.0	3.45	18	64	29	100	0.06	3.84
36	0.06	1.214	1485	1.02	3.42	18.4	63	25	85	0.0612	3.85
37	0.06	1.23	1517	1.04	3.44	16.8	58	21	72	0.0624	3.62
38	0.06	1.244	1546	1.07	3.48	6.4	57	22	76	0.0642	3.66
39	0.06	1.25	1560	1.01	3.45	12.8	44	21	72	0.0606	2.67
40	0.06	1.26	1579	1.1	3.44	13	45	20	69	0.066	2.97
41	0.06	1.348	1768	1.26	3.55	8.2	29	14	50	0.0756	2.19

Table. (Contd.)

Entry	P_0, atm	V, km/s	T, K	P_2, atm	ρ/ρ_0	τ_{lab}, μs	τ_{act}, μs	τ_{lab}^{max}, μs	τ_{act}^{max}, μs	P_s, atm	$\tau_{act}P_s$, μs atm
42	0.06	1.348	1768	1.26	3.55	9	32	12.8	45.5	0.0756	2.42
43	0.06	1.36	1792	1.28	3.56	6.6	23.5	11.2	40	0.0768	1.8
44	0.06	1.397	1878	1.35	3.59	5.4	19.4	8.8	31.6	0.081	1.57
45	0.06	1.429	1952	1.4	3.63	4.2	15.2	8.2	30	0.084	1.28
46	0.06	1.548	2243	1.665	3.7	2.5	9.3	9.7	36	0.1	0.93
47	0.06	1.56	2273	1.7	3.7	3	11	7.5	28	0.102	1.1
48	0.06	1.64	2483	1.87	3.77	1.2	4.5	5.4	20.4	0.112	0.5
$5\%\ (1O_2 + 1H_2) + 95\%Ar\ (2H_2 + O_2) = 3.75\%$											
49	0.06	1.17	1432	0.955	3.33	31	103	41	136	0.0358	3.69
50	0.06	1.185	1462	0.98	3.345	30	100	39	130	0.0367	3.05
51	0.06	1.216	1526	1.03	3.38	21.4	72	25.6	86.5	0.0386	2.8
52	0.06	1.238	1572	1.07	3.4	18.8	64	24	81.6	0.0401	2.57
53	0.06	1.31	1730	1.2	3.47	12	41	18	62	0.045	1.85
54	0.06	1.35	1820	1.28	3.51	8.2	29	13	46	0.048	1.39
$5\%\ (5O_2 + 1H_2) + 95\%\ Ar\ (2H_2 + O_2) = 1.25\%$											
55	0.06	1.06	1225	0.79	3.22	78	251	114	367	0.0099	2.5
56	0.06	1.106	1311	0.862	3.29	53	174	65–93		0.0108	1.88
57	0.06	1.14	1377	0.92	3.33	42	140	56	187	0.0115	1.61
58	0.06	1.196	1488	1.01	3.39	27	91	34.6	117	0.0126	1.15
59	0.06	1.28	1664	1.16	3.48	16.8	58	26	90	0.0145	0.84
60	0.06	1.344	1809	1.28	3.54	10.6	37	17	60	0.016	0.6
61	0.06	1.466	2100	1.53	3.63	6.6	24	11.6	42	0.0191	0.46
62	0.06	1.48	2134	1.56	3.64	6.2	22.6	12	43.7	0.0195	0.44
63	0.06	1.55	2316	1.7	3.686	3.4	12.5			0.0212	0.265
$5\%\ (1O_2 + 4H_2) + 95\%\ Ar\ (2H_2 + O_2) = 3\%$											
64	0.12	0.845	870	0.98	2.81	726	2040	738	2074	0.0294	60
65	0.12	0.85	870	0.98	2.8	816	2285	833	2332	0.0294	67
66	0.12	0.868	900	1.0	2.85	884	2520	912	2600	0.03	75
67	0.12	0.868	900	1.0	2.85	888	2530	920	2622	0.03	76
68	0.12	0.868	900	1.0	2.85	916	2610	940	2680	0.03	78
69	0.12	0.88	914	1.05	2.87	750	2150	770	2210	0.0315	68
70	0.12	0.915	968	1.14	2.95	500	1475	562	1660	0.0342	73
71	0.12	0.926	985	1.17	2.96	532	1574	570	1687	0.0351	55
72	0.09	0.945	1008	0.9	2.99	534	1597	557	1660	0.027	43
73	0.09	0.947	1008	0.91	3.0	576	1728	586	1754	0.0273	47
74	0.12	0.95	1024	1.23	3.0	510	1530	550	1650	0.0369	56.4
76	0.12	1.0	1100	1.36	3.08	170	523	207	637	0.0408	21.3
77	0.12	1.0	1107	1.37	3.08	124	382	139	428	0.0411	15.7
78	0.12	1.0	1114	1.38	3.09	153	472	185	574	0.0414	19.5
79	0.06	1.02	1142	0.71	3.15	189–217	595–683	260	820	0.0213	12.7–14.6
80	0.06	1.02	1142	0.71	3.15	185–212	586–668	277	872	0.0213	12.5–14.2
81	0.12	1.06	1212	1.45	3.15	70	220	94	296	0.0435	9.7
82	0.06	1.06	1212	0.77	3.176	138	438	147	467		10.8
83	0.09	1.08	1250	1.2	3.21	83	266	141	453	0.036	9.6

Table. (Contd.)

Entry	P_0, atm	V, km/s	T, K	P_2, atm	ρ/ρ_0	τ_{lab}, μs	τ_{act}, μs	τ_{lab}^{max}, μs	τ_{act}^{max}, μs	P_s, atm	$\tau_{act}P_s$, μs atm
84	0.06	1.11	1305	0.845	3.25	67	217	86	280	0.0243	5.3
85	0.09	1.11	1305	1.29	3.25	45	146	68	222	0.0387	5.65
86	0.06	1.11	1305	0.845	3.25	65	211	87	282	0.0253	5.3
87	0.06	1.137	1360	0.9	3.27	55	180	78	255	0.027	4.9
88	0.06	1.14	1362	0.9	3.27	55	180	64	209	0.027	4.9
89	0.12	1.141	1364	1.8	3.28	28.6	93.7			0.054	5.06
90	0.12	1.147	1375	1.8	3.28	24.4–31.6	80–103	38	124	0.054	4.3–5.5
91	0.06	1.17	1421	0.94	3.31	45	149	51	169	0.0282	4.2
92	0.06	1.17	1421	0.94	3.31	45.2	150	65	215	0.0282	4.23
93	0.09	1.18	1440	1.43	3.33	32	106	43	143	0.0429	4.54
94	0.09	1.19	1461	1.46	3.34	25	84			0.0438	3.63
95	0.12	1.2	1481	1.98	3.35	15.6	52	24	80	0.0594	3.1
96	0.06	1.2	1491	1.0	3.35	33	110	46	154	0.03	3.3
97	0.09	1.29	1660	1.7	3.43	14.2	48.7	22.2–24	76–83	0.051	2.48
98	0.06	1.295	1681	1.16	3.44	14.8–19.8	51–68	25	86	0.0348	1.8
99	0.06	1.3	1692	1.17	3.44	16	55	29	100	0.0351	1.9
100	0.06	1.31	1714	1.2	3.45	16	55	28	97	0.036	2
101	0.09	1.34	1781	1.86	3.49	10.6	37	13.3	46.5	0.056	2.1
102	0.06	1.336	1841	1.29	3.49	10.8	37.6	20	70	0.039	1.47
103	0.06	1.42	1968	1.4	3.54	11.4	40	28	99	0.042	1.68
104	0.06	1.52	2215	1.6	3.61	6	22	20	72	0.048	1.06
105	0.09	1.52	2215	2.4	3.61	4	14.4			0.072	1.03
106	0.09	1.54	2267	2.47	3.63	4	14.5			0.074	1.07
107	0.06	1.6	2390	1.75	3.66	4	14.6	11	40	0.0525	0.77
108	0.06	1.87	3197	2.4	3.8	~1	~3.8			0.072	0.27
11% ($1O_2 + 10H_2$) + 89% Ar ($2H_2 + O_2$) = 3%											
109	0.12	0.903	890	1.04	2.92	820	2394			0.0312	74.7
110	0.12	0.906	902	1.06	2.94	788	2316	792	2328	0.0318	73.6
111	0.12	0.936	945	1.13	3.0	640	1914	641	1917	0.0339	64.9
112	0.12	0.973	1000	1.23	3.06	484	1481	497	1521	0.0369	54.6
113	0.12	0.98	1011	1.24	3.07	470	1440			0.0372	53.6
114	0.12	1.02	1046	1.29	3.1	266	824	288	893	0.0387	32
115	0.12	1.01	1058	1.32	3.125	204	638	233	728	0.0396	25
116	0.12	1.02	1074	1.35	3.125	130	406	147	460	0.0405	16
117	0.12	1.03	1090	1.38	3.15	153	482	209	658	0.0414	20
118	0.12	1.037	1102	1.4	3.16	94	297	98	310	0.042	12.5
119	0.12	1.07	1156	1.5	3.2	131	420	140	435	0.045	19
120	0.12	1.11	1224	1.47	3.27	70	230	77	265	0.0441	10
121	0.09	1.21	1405	1.44	3.4	36.1	122	42	143	0.0432	5.25
122	0.12	1.33	1641	2.32	3.53	7.6	27	10.4	36.7	0.0696	1.87
123	0.06	1.34	1661	1.18	3.54	18.1	64			0.0354	2.26
124	0.06	1.36	1700	1.2	3.566	16	57			0.036	2.05
125	0.06	1.46	1920	1.4	3.67	9	33	14.6	53.6	0.042	1.39
126	0.06	1.57	2176	1.63	3.72	4.7	17.6	7.4	27.5	0.0485	0.85

Table. (Contd.)

Entry	P_0, atm	V, km/s	T, K	P_2, atm	ρ/ρ_0	τ_{lab}, μs	τ_{act}, μs	τ_{lab}^{max}, μs	τ_{act}^{max}, μs	P_s, atm	$\tau_{act}P_s$, μs atm
127	0.06	1.577	2193	1.64	3.74	4.5	17	7	26	0.0492	0.84
128	0.06	1.6	2323	1.75	3.77	3.05	11.5	7.7	29	0.0525	0.6
129	0.06	1.84	2872	2.24	3.86	1.4	5.4	8	31	0.0672	0.36
130	0.06	1.88	2991	2.34	3.91	~0.8	3.1	4.1	16	0.0702	~0.22
21% ($1O_2 + 20H_2$) + 79% Ar ($2H_2 + O_2$) = 3%											
131	0.12	0.947	870	1.0	3.02	980	2960			0.03	89
132	0.12	1.0	953	1.18	3.1					0.0354	
133	0.12	1.04	997	1.28	3.2	352	1126	382	1222	0.0384	43
134	0.12	1.06	1037	1.32	3.2	212	678	220	700	0.0396	27
135	0.12	1.1	1077	1.42	3.3	170	560	186	614	0.0426	24
136	0.12	1.12	1123	1.47	3.3	88	290	109	360	0.0441	12.8
137	0.06	1.337	1470	1.06	3.62	35.4	128			0.0318	4.1
138	0.12	1.36	1510	2.2	3.6	15.6	56	19	68	0.066	3.7
139	0.12	1.35	1547	2.27	3.68	12.2	45	18	66	0.0681	3.06
140	0.06	1.515	1805	1.37	3.8	8.2	31			0.0411	1.27
141	0.06	1.58	1936	1.5	3.86	4	15.45			0.045	0.7
142	0.06	1.59	1978	1.5	3.87	5	19.35			0.045	0.87
143	0.06	1.634	2050	1.6	3.9	4.8	18.7			0.048	0.9
144	0.06	1.77	2350	1.88	4.0	~1.9	7.3			0.0564	0.41
145	0.06	1.78	2387	1.9	4	2.2	8.8			0.057	0.5
146	0.06	1.79	2397	1.93	4.02	1.8	7.2			0.0579	0.42
147	0.06	1.82	2466	2.0	4.04	2.5	10			0.06	0.6
148	0.06	1.866	2576	2.1	4.08	~1.3	5.3			0.063	0.2

Note: P_0 is the initial pressure of the mixture examined; P_2 is the gas pressure behind the shock front; T is the gas temperature behind the shock front; V is the shock wave velocity; ρ/ρ_0 is the density drop across the shock front; τ_{lab} and τ_{lab}^{max} are the ignition delay times in the laboratory coordinate system, measured as the onset and maximum points of the signal, respectively; τ_{act} and τ_{act}^{max} are the actual ignition delay times associated with the shock front, measured as the onset and maximum points of the signal, respectively; P_s is the pressure of the stoichiometric part of the combustible mixture.

increase, τP_s also increases, so τ is no longer a linear function of $1/P_s$.

Note the limitation that arises in ignition delay measurements for shock waves in shock tubes at low temperatures. Figure 5 plots our temperature-dependent τ data for the 1% O_2 + 4% H_2 + 95% Ar mixture at temperatures of 900 to 2400 K and pressures of 0.7 to 2.5 atm, as well as the lengths of the shock-heated and -compressed gas plug. The plug length was derived from light absorption by dioxygen (Schumann–Runge band, λ = 220 nm) and, in special-purpose experiments, from hydrogen ignition in the contact zone upon mixing of hydrogen with the 6% O_2 + 94% Ar mixture. The data obtained by these two methods almost coincide.

As is clear from Fig. 5, at 900–1000 K the ignition delay time for the mixture examined is so long that the ignition zone adjoins the contact zone separating the driver gas and the mixture. Therefore, for reliable τ measurements below 1000 K in incident shock waves, it is necessary to monitor the position of the ignition zone relative to the contact zone and to choose experimental conditions correspondingly. In this situation, it is seemingly preferable to use reflected shock waves or longer shock tubes.

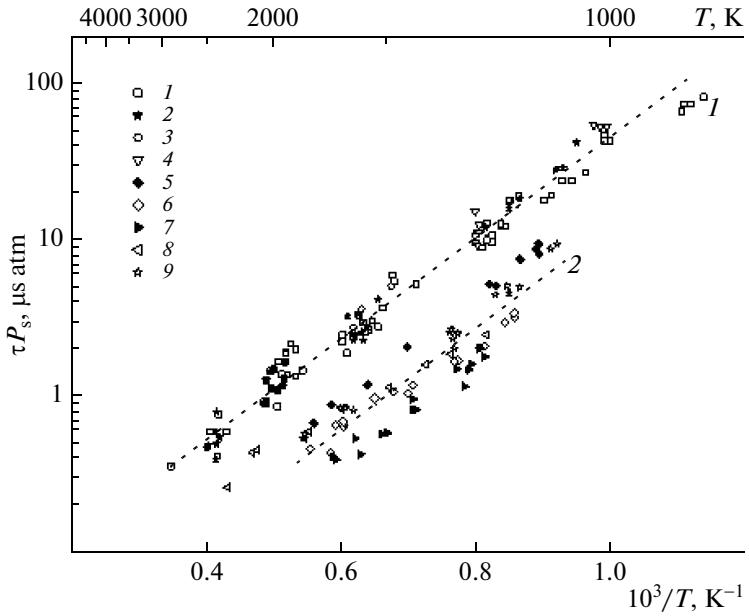

Fig. 3. Temperature dependences of τP_s measured in this work and calculated from data of other authors [7–11] for H_2–O_2–Ar mixtures of different compositions for $P = 0.5$–64 atm. $P_s = 0.02$–0.1 atm, and $T = 900$–3000 K: (*1*) this work; (*2*) [7]; (*3*) [8]; (*4*) [9]; (*5*) [10], $H_2/O_2 = 1.0$; (*6*) [10], $H_2/O_2 = 0.25$; (*7*) [10], $H_2/O_2 = 0.125$; (*8*) this work, $H_2/O_2 = 0.2$; (*9*) [11], $H_2/O_2 = 0.5$. (*1–4*) Lean mixtures and (*5–9*) rich mixtures.

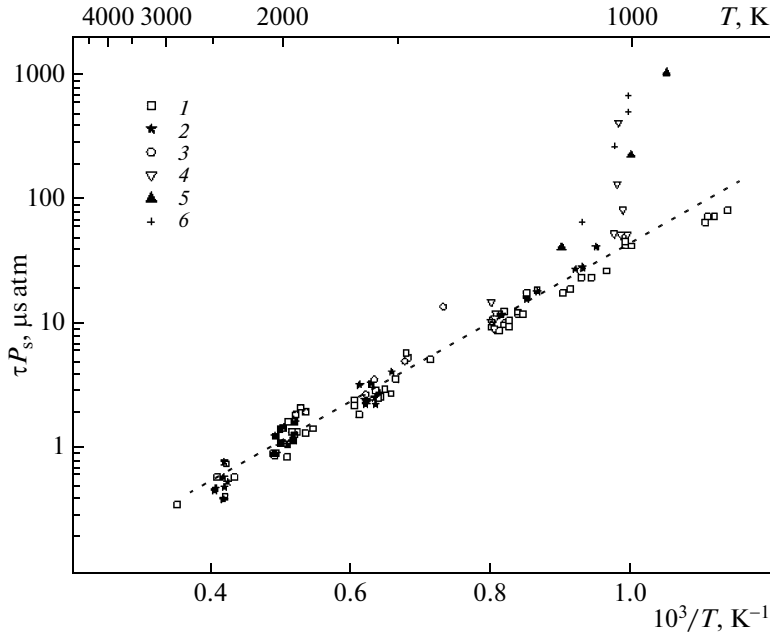

Fig. 4. Comparison of the data of this work and from [7, 8] to the data from [9, 12, 13] for $P_s = 0.05$–0.44 atm and $P = 1$–7 atm: (*1*) this work, (*2*) [7], (*3*) [8], (*4*) [9], (*5*) [12], and (*6*) [13].

CONCLUSIONS

The $^{\cdot}OH$ radical formation delay time τ was measured for the ignition of hydrogen–oxygen mixtures diluted with argon (79–97%) in incident shock waves over wide ranges of mixture composition (H_2/O_2 = 20–0.125), temperature ($T = 900$–3000 K), and pressure ($P = 0.5$–2.5 atm), with the pressure of the stoichiometric part of the combustible mixture being $P_s <$ 0.1 atm. It was discovered that τ depends linearly on $1/P_s$ for any mixture. This allowed us to convert the

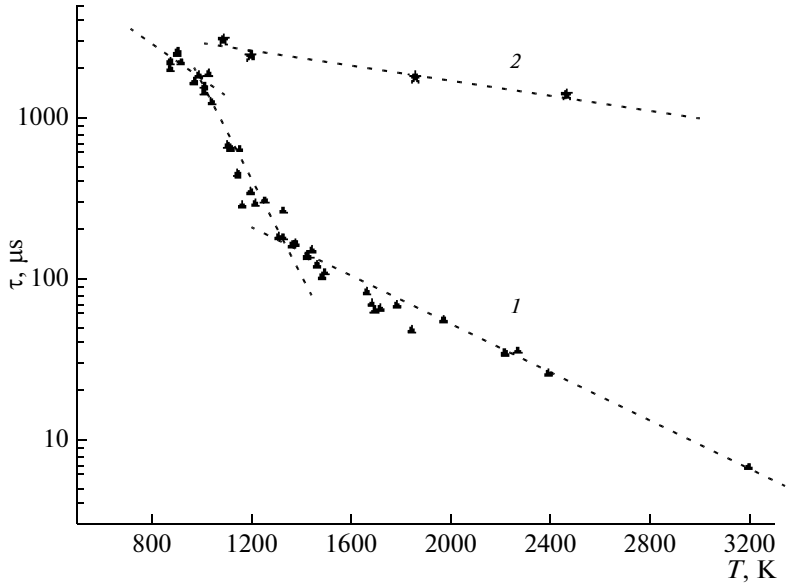

Fig. 5. Temperature dependences of (*1*) the ignition delay time and (*2*) the length of the plug of the shock-heated gas in units of time for the 5% (O_2 + 4H_2) + 95% Ar mixture.

experimental τ data from the above conditions to normal pressure.

The conversion of the experimental τ data to normal pressure applied to the stoichiometric part of the combustible mixture (P_s) made it possible to describe the data obtained in this work and in other studies [7–11] in terms of a common Arrhenius plot at $T = 900$–3000 K, $P = 1$–64 atm, and $P_s = 0.02$–0.1 atm, irrespective of the H_2/O_2 ratio (20–0.152) and argon content.

At $T \approx 1000$ K, $P_s > 0.1$, and $P > 2$ atm, for rich mixtures relationship (1) based on converted data taken from [9, 12, 13] is invalid and τ increases sharply with increasing P and P_s.

At low temperatures (large τ values), the accuracy of the determination of the ignition delay time for combustible mixtures in a shock tube is limited by the interaction between the ignition zone and the turbulent contact zone of the driver gas. This leads to underestimation of τ at low temperatures (Fig. 5) and makes it difficult to measure large τ values in incident shock waves.

ACKNOWLEDGMENTS

The authors are grateful to O.V. Skrebkov for the initiation of this study and to P.V. Kozlov for helpful consultations.

This study was supported by the Russian Foundation for Basic Research, grant no. 08-03-01034a).

REFERENCES

1. Semenov, N.N., *O nekotorykh problemakh khimicheskoi kinetiki i reaktsionnoi sposobnosti* (Topics in Chemical Kinetics and Reactivity), Moscow: Akad. Nauk SSSR, 1958.
2. Kondrat'ev, V.N. and Nikitin, E.E., *Kinetika i mekhanizm gazofaznykh reaktsii* (Kinetics and Mechanism of Gas-Phase Reactions), Moscow: Nauka, 1974.
3. *Teoriya goreniya i vzryva* (Combustion and Explosion Theory), Moscow: Nauka, 1981.
4. Smekhov, G.D., Ibragimova, L.B., Karkach, S.P., Skrebkov, O.V., and Shatalov, O.P., *Teplofiz. Vys. Temp.*, 2007, vol. 45, no. 3, p. 440 [*High Temp.* (Engl. Transl.), vol. 45, no. 3, p. 395].
5. Popov, N.A., *Teplofiz. Vys. Temp.*, 2007, vol. 45, no. 2, p. 296 [*High Temp.* (Engl. Transl.), vol. 45, no. 2, p. 261].
6. Skrebkov, O.V. and Karkach, S.P., *Kinet. Katal.*, 2007, vol. 48, no. 3, p. 388 [*Kinet. Catal.* (Engl. Transl.), vol. 48, no. 3, p. 367].
7. Ryu, S. and Hwang, S., *J. Phys. Chem.,* 1995, vol. 99, p. 13984.
8. Petersen, E.L., Davidson, D.F., Rohrig, M., and Hanson, R.K., *Proc. 20th Int Symp. on Shock Waves*, Pasadena, 1995, p. 941.
9. Cohen, A. and Larsen, J., *Report BRL*, 1967, no. 1386.
10. Jachimowski, C.J. and Houghton, W.M., *Combust. Flame*, 1971, vol. 17, p. 25.
11. Schott, G.L. and Kinsey, J.L., *J. Chem. Phys.*, 1958, vol. 29, p. 1177.
12. Pang, G.A., Davidson, D.F., and Hanson, R.K., *Proc. Combust. Inst.*, 2009, vol. 32, p. 181.
13. Skinner, G.B. and Ringrose, G.H., *J. Chem. Phys.*, 1966, vol. 42, p. 2190.
14. Pavlov, V.A., *Fiz.-Khim. Kinet. Gaz. Dinam.*, 2009, vol. 8 (www.chemphys.edu.ru).